

Junction formation by Zn(O,S) sputtering yields CIGSe-based cells with efficiencies exceeding 18%

R. Klenk*, A. Steigert, T. Rissom, D. Greiner, C.A. Kaufmann, T. Unold and M.C. Lux-Steiner

Helmholtz-Zentrum-Berlin für Materialien und Energie, Hahn-Meitner-Platz 1, D14109 Berlin, Germany

Abstract

In an effort to reduce the complexity and associated production costs of CIGSe-based solar cells, the commonly used sputtered un-doped ZnO layer has been modified to eliminate the requirement for a dedicated buffer layer. After replacing the ZnO target with a mixed ZnO/ZnS target, efficient solar cells could be prepared by sputtering directly onto the as-grown CIGSe surface. This approach has now been tested with high quality lab-scale glass/Mo/CIGSe substrates. An efficiency of 18.3% has been independently confirmed without any post deposition annealing or light-soaking.

Keywords

Cu(In,Ga)Se₂, Zn(O,S), thin film, hetero junction, buffer, sputtering

*Correspondence

Reiner Klenk, E-IH, Helmholtz-Zentrum für Materialien und Energie, Hahn-Meitner-Platz 1, D14109 Berlin, Germany.

E-mail: klenk@helmholtz-berlin.de

Introduction

The standard CIGSe solar cell is a heterojunction following the absorber/window concept. The window consists of three wide-bandgap layers, each dedicated to fulfill a specific requirement. After junction formation by the buffer layer, the undoped ZnO (i-layer) reduces the influence of inhomogeneities and pin holes, whereas the highly doped ZnO transports the generated photo current laterally to the grid finger or module interconnect. This concept of one layer per function allows for a certain degree of independent optimization and has resulted in robust processes for high efficiency small area cells as well as large scale module production. On the other hand, if a layer were to serve more than a single purpose, the cell structure could be simplified with significant benefits regarding manufacturing costs. Using a structure without a dedicated buffer layer appears to be particularly attractive as its deposition often involves problematic liquids or gases and tends to be a slow process. It has been argued that, besides establishing a suitable band line-up and Fermi-level position at the interface, the buffer layer also “protects” the heterojunction during sputtering of ZnO. Following that argument it ought to be deposited by “soft” processes such as chemical bath deposition or chemical vapor deposition. Nevertheless, sputtering directly onto the absorber has been attempted previously using ZnO [1] or (Zn,Mg)O [2] with some success. On the other hand, junction formation through Zn(O,S) prepared by soft methods is well known to result in excellent efficiencies [3]. Hence the idea that using Zn(O,S) rather than ZnO for i-layer sputtering might eliminate the requirement for a separate buffer layer. Partially reactive sputtering [4] or sputtering from two binary targets [5] were first steps to determine material properties and band line-up [6] and to compare them to literature data [7,8]. In a next step we moved to a single mixed target to more closely match the currently used conditions for i-layer sputtering and demonstrated efficiencies in the 14-15% range using absorbers from industrial production [9]. The purpose of the work described in the following has been to demonstrate the

efficiency potential of this approach by using high quality lab-scale absorbers prepared by multi stage co-evaporation.

Experimental

The CIGSe absorber was prepared by multi stage co-evaporation [10]. The substrate was a sodium containing glass with extended temperature stability (SCHOTT EtaMax [11]). The glass was cleaned in an ultrasonic bath using acetone, isopropanol and purified water. Sputtered molybdenum was used as back contact. The multi stage process was controlled by light scattering similar to the approach described in [12]. While selenium was evaporated continuously during the whole duration of the process, the fluxes of copper, indium and gallium were controlled using shutters and adjustment of the source temperatures. For the formation of an In-Ga-Se precursor, alternating layers of Ga-Se and In-Se were evaporated (2 layers each, starting with Ga-Se, substrate temperature 330 °C). After that, the substrate temperature was raised to 610°C nominally and Cu-Se was evaporated in a second stage. When the film reached the point of stoichiometry, we observed a steep increase in the scattered laser light (formation of Cu_xSe phases). The duration from the beginning of the second stage until this point of stoichiometry was measured and the Cu-Se evaporation was continued for a further 16% of that duration. This was followed by evaporation of selenium only for two minutes and then co-evaporation of indium, gallium and selenium. Evaporation rates and duration were adjusted for a nominal final $[\text{Cu}]/([\text{In}]+[\text{Ga}])$ ratio of 0.83. Finally, a small amount of In-Se was evaporated as described in [13]. During cool-down, the selenium flux was maintained until the sample reached a temperature of 250°C.

After cool down the absorber substrate was removed from the evaporator and transferred in air to the sputtering system. The sample was exposed to ambient conditions for about one hour. No intermediate surface conditioning procedures were applied. The Zn(O,S) was RF-sputtered (13.56 MHz) from a mixed target (diameter 125 mm) with an argon pressure of 5 μBar . The target was obtained from a commercial supplier with a nominal $[\text{ZnS}]/([\text{ZnO}]+[\text{ZnS}])$ ratio of 25%. The deposition was carried out with a power density of 1.6 W/cm^2 at the target surface without deliberate substrate heating. To investigate the homogeneity across the deposition area, a film with 400 nm thickness was deposited and the composition measured by energy dispersive X-ray spectroscopy (EDX). For solar cell preparation, the deposition period was 70 seconds (film thickness \approx 60 nm). After that the sample was again transferred in air to a different sputtering system for the deposition of standard highly doped ZnO:Al with a thickness of 240 nm and sheet resistance of 30 Ω/\square . A contact grid consisting of Ni/Al was evaporated through a shadow mask. 32 cells with total areas of 0.5 cm^2 on a 5x5 cm^2 substrate were defined by mechanical scribing. A single layer MgF_2 anti-reflective coating with a thickness of 110 nm was deposited by evaporation. There were no additional annealing steps between or after processes. Current voltage characteristics were measured without light-soaking, in-house and independently by ISE Freiburg (simulated AM 1.5 conditions). The quantum efficiency was measured without voltage or light bias with the beam focused in-between grid fingers.

Results

In our previous work [9] we had used a target with significantly higher sulfur content but had speculated that this composition was at the border of the process window (current blocking by a conduction band spike $>$ 0.3 eV [6,14]) for deposition on as-grown absorber surfaces. The sulfur content in the target has been reduced for this work and current blocking in cells was indeed no longer observed. The sulfur content in the film (19%-22%) is slightly lower than expected from the target composition (25%), in particular towards the edges of the deposition area as shown by the EDX scan in Fig. 1. Judging from X-ray diffraction and optical transmission the films are single phase Zn(O,S). The

first test on lab-scale absorbers yielded a substrate where 16 of the 32 cells had efficiencies above 17%. The best cell on the substrate had an efficiency of 18.3% in excellent agreement of the in-house and ISE measurements (Fig. 2). The quantum efficiency is shown in Fig. 3. There are some features in the long wavelength cutoff which we do not typically observe clearly in cells with CdS buffer but had seen already with reactively sputtered Zn(O,S) on the same type of absorber [15]. Optical modeling and reflectance measurements (not shown here) suggest that these are interference fringes and not related to the absorption coefficient of the absorber. Distribution of the cell performance across the substrate (Fig. 4) suggests a superposition of absorber as well as buffer layer inhomogeneity.

Discussion

Once junction formation has succeeded in sufficiently reducing interface recombination, the cell efficiency is determined by absorber properties. In particular, the gallium content determines the absorber band gap and can therefore lead to different open circuit voltages. Hence, it is not straightforward to rate the performance of the sputtered Zn(O,S) by comparing it to literature data [3,16]. Nevertheless, the data listed in Table 1 show that the results achieved in this work compare very well to the overall best cell previously prepared by using dry processes only [3]. There still is a small gap with respect to the best cell with chemical bath deposited (CBD) Zn(O,S) buffer and to our best cell with standard CBD CdS [17]. A CdS-buffered reference cell with an absorber from the same run was also prepared in this work, however, it showed an efficiency of only 16.2%. This indicates a problem in processing and makes the direct comparison invalid.

While the homogeneity is certainly already quite good considering the small area lab-scale deposition systems, a closer look at the remaining trends may give hints concerning the process parameter window. In our previous work, the fill factor was often lower in the center of the substrate, *i.e.* the best cells were at the edge of the substrate where the sulfur content of the Zn(O,S) layer was slightly lower. This was tentatively explained by the onset of current blocking by a conduction band spike at the interface. Here, with the new target with significantly smaller sulfur content overall, the best cells are observed in the center of the substrate. It is conceivable that, at least for this particular type of absorber, we are now at the lower boundary of the parameter window (with respect to sulfur content) where the band alignment switches from spike to cliff [6] and where the band bending in the absorber is reduced. In addition, the open circuit voltages are lower at the left edge of the substrate (Fig. 4) as compared to the right edge which implies imperfect rotational symmetry of the Zn(O,S) deposition or a slight inhomogeneity of the absorber.

Conclusions

In summary, our work further strengthens the assumption that Zn(O,S) is indeed one of the best Cd-free materials for forming junctions with chalcopyrites. Our new record efficiency for junctions formed by sputtering also supports the assumption that soft preparation methods for buffer preparation are not mandatory. This opens up a very attractive route to Cd-free chalcopyrite based modules using sputter deposited window layers without a dedicated buffer. Further work needs to investigate the feasibility of large area deposition and long term module stability.

Acknowledgements

This work has partially been funded by the German federal ministry of education and research (NeuMaS, contract 13N11768) and by the German federal ministry for the environment, nature conservation and nuclear safety (comCIGS II, contract 0325448D). We thank W. Mannstadt (SCHOTT AG) for discussions and providing the glass substrates. Technical support by C. Ferber, P. Gerhardt, M.

Kirsch, and J. Lauche is gratefully acknowledged.

References

- 1 Ramanathan K, Hasoon FS, Smith S, Young DL, Contreras MA, Johnson PK, Pudov AO, Sites JR. Surface treatment of CuInGaSe₂ thin films and its effect on the photovoltaic properties of solar cells. *Journal of Physics and Chemistry of Solids* 2003; **64**: 1495-1498.
- 2 Glatzel Th, Steigert H, Sadewasser S, Klenk R, Lux-Steiner MC. Potential distribution of Cu(In,Ga)(S,Se)₂ -solar cell cross-sections measured by Kelvin probe force microscopy. *Thin Solid Films* 2005; **480**: 177-182, DOI: 10.1016/j.tsf.2004.11.065.
- 3 Zimmermann U, Ruth M, Edoff M. Cadmium-free CIGS mini-modules with ALD-grown Zn(O,S)-based buffer layers : Proceedings of the 21st European Photovoltaic Solar Energy Conference, Dresden 2006; 1831-1834.
- 4 Grimm A, Kieven D, Klenk R, Lauermann I, Neisser A, Niesen T, Palm J. Junction formation in chalcopyrite solar cells by sputtered wide gap compound semiconductors. *Thin Solid Films* 2011; **520**: 1330-1333
- 5 Okamoto A, Minemoto T, Takakura H. Application of Sputtered ZnO_{1-x}S_x Buffer Layers for Cu(In,Ga)Se₂ Solar Cells. *Japanese Journal of Applied Physics* 2011; **50**: 04DP10-1 – 04DP10-4, DOI: 10.1143/JJAP.50.04DP10
- 6 Kieven D, Grimm A, Lauermann I, Lux-Steiner MC, Palm J, Niesen T, Klenk R. Band alignment at sputtered ZnS_xO_{1-x}/Cu(In,Ga)(Se,S)₂ heterojunctions. *Physica Status Solidi (RRL)* 2012; **6**: 294-296, DOI: 10.1002/pssr.201206195
- 7 Meyer BK, Polity A, Farangis B, He Y, Hasselkamp Th, Krämer Th, Wang C. Structural properties and bandgap bowing of ZnO_{1-x}S_x thin films deposited by reactive sputtering. *Applied Physics Letters* 2004; **85**: 4929-4931
- 8 Persson C, Platzer-Björkman C, Malmström J, Törndahl T, Edoff M. Strong Valence-Band Offset Bowing of ZnO_{1-x}S_x Enhances p-Type Nitrogen Doping of ZnO-like Alloys. *Physical Review Letters* 2006; **97**: 146403-1 – 146403-4, DOI: 10.1103/PhysRevLett.97.146403
- 9 Grimm A, Kieven D, Lauermann I, Lux-Steiner MC, Hergert F, Schwieger R, Klenk R. Zn(O, S) layers for chalcopyrite solar cells sputtered from a single target. *EPJ Photovoltaics* 2012; **3**: 30302-p1 – 30302-p4, DOI: 10.1051/epjpv/2012011
- 10 Caballero R, Kaufmann CA, Efimova V, Rissom T, Hoffmann V, Schock HW. Investigation of Cu(In,Ga)Se₂ thin-film formation during the multi-stage co-evaporation process. *Progress in Photovoltaics: Research and Applications* 2013; **21**: 30-46.
- 11 Mannstadt W, Rudigier-Voigt E, Wolff S, Kuhr M, Schmitt S, Scheumann V, Rissom T, Kaufmann CA, Schock HW. New glass substrates enabling high performance CIGSe cells. Proceedings of the 25 th European Photovoltaic Solar Energy Conference, Valencia 2010, 3516-3518.
- 12 Kaufmann CA, Neisser A, Klenk R, Scheer R. Transfer of Cu(In,Ga)Se₂ thin film solar cells to flexible substrates using an in-situ process control. *Thin Solid Films* 2005; **480**: 515-519.
- 13 Repins I, Contreras MA, Egaas B, Dehart C, Scharf J, Perkins CL, To B, Noufi R. 19.9%- efficient ZnO/CdS/CuInGaSe₂ solar cell with 81.2% fill factor. *Progress in Photovoltaics: Research and Applications* 2008; **16**: 235–239.
- 14 Niemegeers A, Burgelman M, de Vos A. *Applied Physics Letters* 1995; **67**: 843-845
- 15 Grimm A, Just J, Kieven D, Lauermann I, Palm J, Neisser A, Rissom T, Klenk R. Sputtered Zn(O,S) for junction formation in chalcopyrite-based thin film solar cells . *Physica Status Solidi (RLL)* 2010; **4**: 109-111, DOI 10.1002/pssr.201004083
- 16 Nakamura M, Kouji Y, Chiba Y, Hakuma H, Kobayashi T, Nakada T. Achievement of 19.7% efficiency with small-sized Cu(InGa)(SeS)₂ solar cells prepared by sulfurization after selenization process with Zn-based buffer. Proceedings of the 39th IEEE Photovoltaic Specialists Conference, Tampa 2013, in press.
- 17 Haarstrich J, Metzner H, Oertel M, Ronning C, Rissom T, Kaufmann CA, Unold T, Schock HW, Windeln J, Mannstadt W, Rudigier-Voigt E. Increased homogeneity and open-circuit voltage of Cu(In,Ga)Se₂ solar cells due to higher deposition temperature. *Solar Energy Materials and Solar Cells* 2011; **95**: 1028-1030.

Tables

Table 1: Parameters of solar cells with differently prepared Zn(O,S) layers.

Absorber	Junction	Voc (mV)	jsc (mA/cm ²)	ff (%)	η (%)
HZB (this work)	Sputtered Zn(O,S)	654	38.4	72.8	18.3
Uppsala U. [3]	ALD Zn(O,S)	689	35.5	75.8	18.5
Solar Frontier [16]	CBD Zn(O,S)	683	37.1	77.8	19.7

Figures

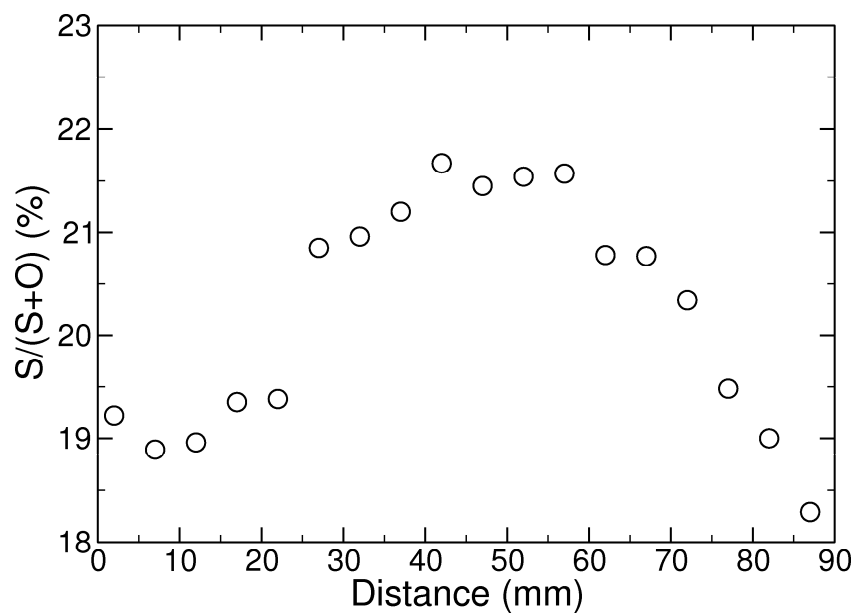


Fig. 1: Composition of a 400 nm Zn(O,S) film measured by EDX diagonally across the circular deposition area.

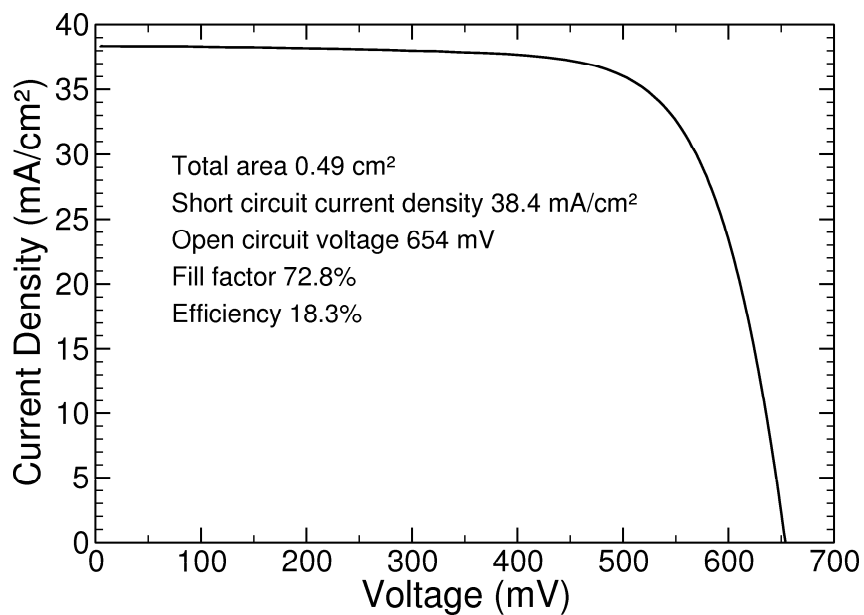


Fig. 2: Current-voltage curve of a Cu(In,Ga)Se₂/Zn(O,S)/ZnO:Al/MgF₂ solar cell as measured by ISE Freiburg.

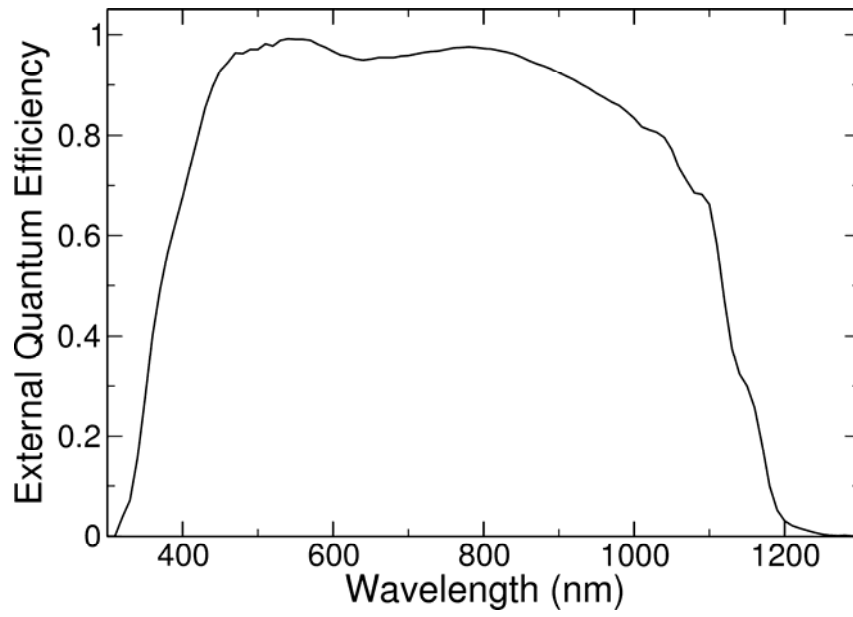


Fig. 3: Active area external quantum efficiency of a $\text{Cu(In,Ga)Se}_2/\text{Zn(O,S)}/\text{ZnO:Al}/\text{MgF}_2$ solar cell.

15.5	16.5	16.7	15.8
16.2	17.5	17.8	17.2
16.1	17.7	18	17.2
16.7	17.8	18.2	17.5
16.6	17.7	18.3	17.7
16.2	17.6	17.9	17.2
16.2	17.7	18.2	17.6
15	17.1	17.7	17

Efficiency (%)

606	623	622	615
621	640	642	633
626	649	649	639
629	652	653	644
628	652	656	648
624	652	653	646
619	648	652	645
600	635	646	638

Open Circuit Voltage (mV)

69.1	70.2	70.5	68.5
70.5	72	72.2	71.4
69.9	72.6	72.6	71.3
71.9	72.6	72.6	72.2
71	72.7	72.9	71.9
71.3	73	72.5	71
70.6	72.7	72.8	71.8
69.2	72.9	72.3	70.9

Fill Factor (%)

Fig. 4: Distribution of cell parameters on a 5x5 cm² substrate with 32 cells (In-house measurements).